New Journal of Physics
The open access journal at the forefront of physics
Deutsche Physikalische Gesellschaft DPG | IOP Institute of Physics

Isotopically varying spectral features of silicon-vacancy in diamond

Andreas Dietrich[1], Kay D Jahnke[1], Jan M Binder[1], Tokuyuki Teraji[2], Junichi Isoya[3], Lachlan J Rogers[1] and Fedor Jelezko[1]

[1] Institute for Quantum Optics and IQST, Ulm University, D-89081 Ulm, Germany
[2] National Institute for Materials Science, 1-1 Namiki, Tsukuba, Ibaraki 305-0044, Japan
[3] Research Center for Knowledge Communities, University of Tsukuba, 1-2 Kasuga, Tsukuba, Ibaraki 305-8550, Japan
E-mail: lachlan.j.rogers@quantum.diamonds

Received 25 July 2014, revised 7 October 2014
Accepted for publication 8 October 2014
Published 11 November 2014

New Journal of Physics **16** (2014) 113019

doi:10.1088/1367-2630/16/11/113019

Abstract

The silicon-vacancy centre (SiV^-) in diamond has exceptional spectral properties for single-emitter quantum information applications. Most of the fluorescence is concentrated in a strong zero phonon line (ZPL), with a weak phonon sideband extending for 100 nm that contains several clear features. We demonstrate that the ZPL position can be used to reliably identify the silicon isotope present in a single SiV^- centre. This is of interest for quantum information applications since only the ^{29}Si isotope has nuclear spin. In addition, we show that the sharp 64 meV phonon peak is due to a local vibrational mode of the silicon atom. The presence of a local mode suggests a plausible origin of the measured isotopic shift of the ZPL.

Keywords: silicon vacancy center, diamond, isotope, local vibrational mode, phonon sideband, ZPL, silicon

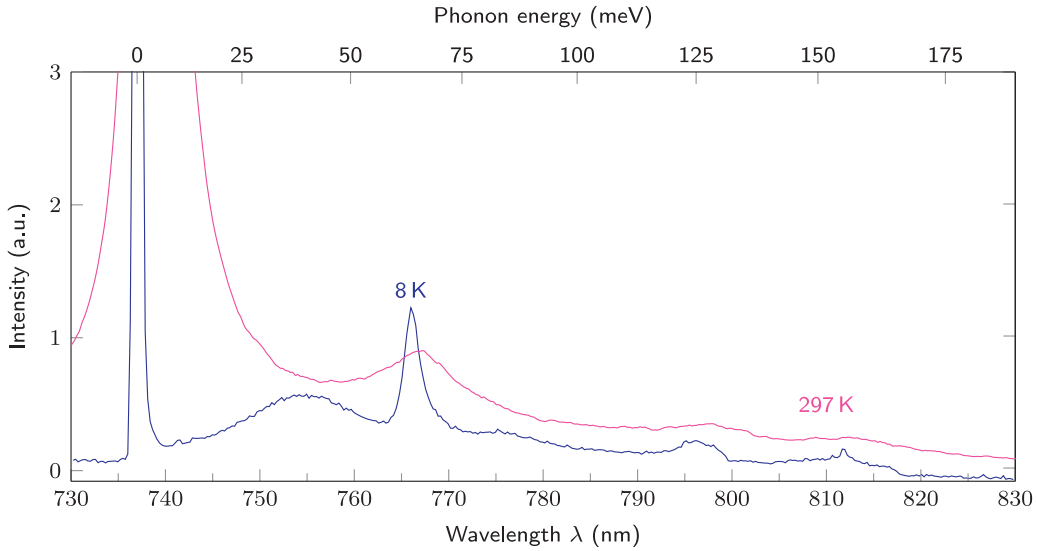

Figure 1. Typical photoluminescence spectra from a single SiV^- site at room and cryogenic temperatures. The strong ZPL at 737 nm contains 70% (65%) of the emission at room (cryogenic) temperature. The sideband shows a number of features, including a prominent narrow line at about 766 nm which is 64 meV from the ZPL.

1. Introduction

Colour centres in diamond provide attractive architectures for quantum information science and quantum metrology. Some are bright enough to be detected at the single-site level [1, 2], and therefore are candidates for single photon generation [3, 4], quantum information processing [5–7], nano-scale sensing [8, 9] and bio-marking [10, 11]. The negative silicon-vacancy (SiV^-) centre is one of the defects in diamond which has shown potential as an exceptional source for single photon applications [12, 13]. Indeed, multiple SiV^- centres have recently been demonstrated to produce indistinguishable photons without needing to be externally tuned into resonance with each other [4, 14]. SiV^- centres are well suited to single photon generation since 70% of their fluorescence is concentrated in a strong zero phonon line (ZPL) and the phonon sideband is weak. A typical photoluminescence spectrum is shown in figure 1.

Recent steps towards optical access of the SiV^- spin have raised the exciting possibility of a usable qubit system being combined with these excellent optical properties [15, 16]. Studies of the related nitrogen-vacancy (NV^-) centre in diamond have demonstrated that optical control of the electronic spin can provide access to nuclear spins of ^{13}C atoms in the lattice [17] and ^{15}N atoms forming the defect site [18]. Nuclear spins have superior coherence properties and are ideal for quantum information processing applications [19]. The most abundant isotope of silicon (^{28}Si) has no nuclear spin, but ^{29}Si is known to have a nuclear spin $I = 1/2$. Here we measure photoluminescence spectra for individual SiV^- defect sites and identify differences that correspond to the silicon isotope. Our results demonstrate the ability to spectrally determine the silicon isotope contained in a single SiV^- centre, providing an important technique to find individual nuclear spins.

Progress towards these exciting spin applications also depends on a substantial understanding of the SiV^- centre. Despite a number of recent advancements [20–23], many fundamental aspects of the SiV^- centre have not been explained. Although the SiV^- sideband is

weak, recent polarization results have suggested interesting physics is displayed in the phonon peaks [23]. In this work we examine the sideband for each of the three stable silicon isotopes, and show that the sharp phonon peak at 766 nm (64 meV) is due to a local vibrational mode involving axial oscillation of the silicon atom. This result resolves contention about the nature of this sideband feature. It is also consistent with the split-vacancy structure (D_{3d} symmetry) proposed for SiV^- [24], further justifying its broad acceptance [22, 23]. In addition, the observed local mode is able to explain the origin of the ZPL isotopic shift.

2. Experimental design

Clark *et al* [25] reported 12 lines in the ZPL structure for a SiV^- ensemble at cryogenic temperatures. This was interpreted as a four-line pattern repeated three times corresponding to the three stable isotopes of silicon. This isotopic shift suggests it should be possible to identify which silicon isotope is present in an individual SiV^- centre. However, many of the early single-site measurements of SiV^- were performed in nanodiamonds and showed large site-to-site variation in the SiV^- spectrum [21]. To date this large inhomogeneous distribution has prevented any reliable spectral identification of the silicon isotope contained in individual SiV^- centres. Recently, much more uniform spectra were reported for single SiV^- sites in high-purity bulk diamond [4]. That same diamond sample was used for the present study, and the narrow inhomogeneous spectral distribution of SiV^- centres made it possible to measure the isotopic shift for individual defect sites.

The SiV^- centres were incorporated into a microwave-plasma chemical vapour deposition (CVD) layer during growth. The single crystal CVD layer was grown on a {001} surface of a low-strain high-pressure high-temperature (HPHT) diamond substrate. Silicon was introduced into the plasma as it etched a 6H-SiC plate placed on the sample mount, and this process assured a natural abundance of silicon isotopes. The silicon incorporated during diamond growth produced SiV^- sites at a density of about 1.5 sites per μm^3 at the measurement depth of 2–3 μm. This density is low enough to resolve single sites in the confocal microscope, but is still high enough to make it convenient to examine a large number of SiV^- sites.

The diamond sample was mounted on the cold finger of a continuous-flow helium cryostat, and cooled to about 8 K. The CVD layer was imaged using a home-built confocal microscope, which had a scan range of 200 × 200 μm. The objective had a numerical aperture of 0.95 and a magnification of 100×. Excitation was provided by 532 nm CW laser with about 1 mW of power at the objective. Fluorescence from SiV^- was measured using avalanche photo diodes (APD). Low resolution spectra covering the entire sideband were measured using a spectrometer with a 150-grooves-per-mm grating. The ZPL was measured with a 1200-grooves-per-mm grating which gave a 16 GHz resolution capable of resolving the four fine-structure lines separated by 50 GHz and 200 GHz.

3. Observing the isotopic shift of spectral features

Photoluminescence (PL) spectra were recorded for 817 individual SiV^- defect sites at a resolution capable of resolving the ZPL fine structure as shown in figure 2(a). Since the 16 GHz linewidth is known to be instrument limited [4], the peaks were fitted with Gaussian functions that allowed line position to be determined with a typical confidence interval of 0.004 nm

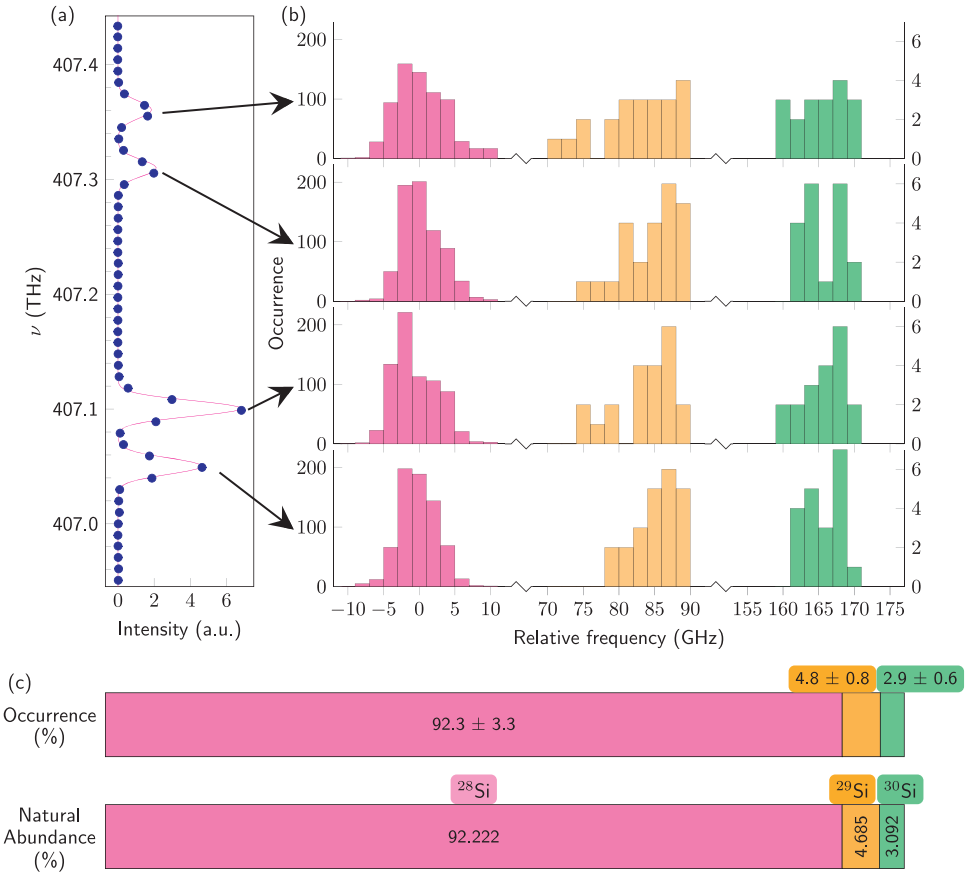

Figure 2. Individual SiV^- ZPLs form clusters matching the natural abundance of the silicon isotopes. (a) Example spectrum of the ZPL for a single SiV^- defect, showing the fine structure recorded with the spectrometer. (b) Histograms showing the distribution of position for each fine-structure line of the ZPL. For each line there is strong bunching into three distinct clusters. The gap between clusters (about 80 GHz) is much larger than the width of each cluster (about 8 GHz) and there were no instances of lines located in between clusters. Each individual site falls into the same coloured cluster for all four of its fine-structure lines. The right-hand vertical axis applies to the centre and right clusters. (c) 754 sites were contained in the first cluster, 39 in the second, and 24 in the third. These occurrences match the natural abundance ratios of the three stable silicon isotopes.

(2 GHz). Figure 2(b) presents histograms of the single-site line positions binned in intervals of 2 GHz. All four of the fine-structure lines show the SiV^- sites naturally clustered into three distinct groups spectrally separated by about 80 GHz. Each individual site had all four of its lines in just one of these three clusters, and there were no sites measured with line positions in between these clusters.

Most SiV^- sites were contained in the shortest wavelength cluster, which was found to have an inhomogeneous distribution of about 8 GHz full-width at half maximum (FWHM). This is an order of magnitude narrower than the 80 GHz separation between the clusters, and so the clustering must arise from a physical effect and cannot be due to spectral noise. The two clusters displaced to longer wavelength occurred less frequently. The number of sites in each of these three clusters corresponds closely to the natural abundance of silicon isotopes as illustrated in figure 2(c). It is concluded that the displacement between clusters must arise from changing the

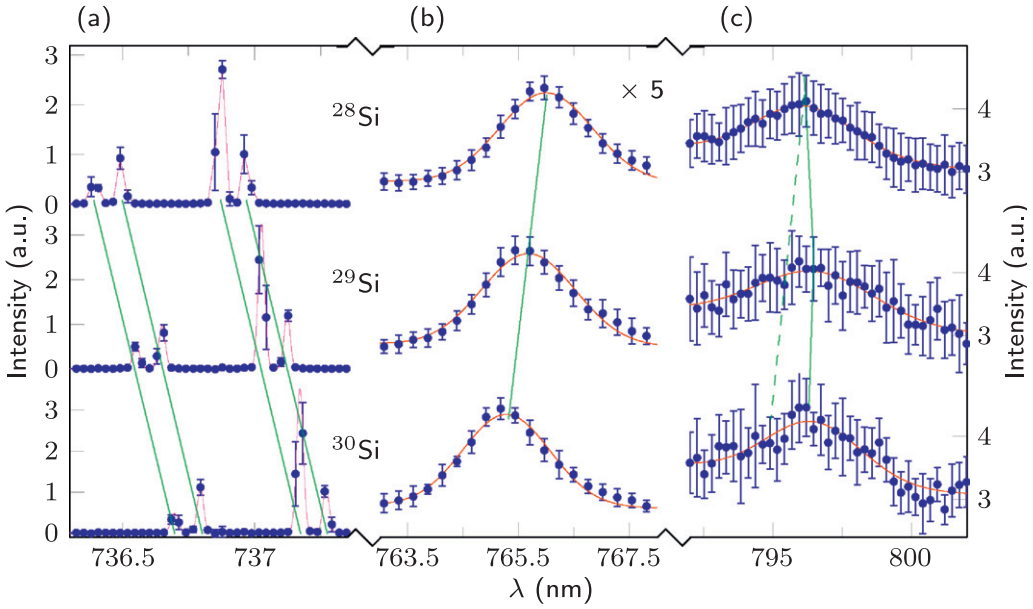

Figure 3. Two features in the SiV$^-$ photoluminescence band shift systematically with silicon isotope. (a) The ZPL shifts to longer wavelength as the silicon atom increases in mass, by 0.16 nm (87 GHz) and 0.30 nm (166 GHz) for ^{29}Si and ^{30}Si respectively. These fine structure lines were fitted with Gaussian shapes since their width is instrument limited. (b) The sharp phonon peak at 766 nm moves to shorter wavelengths as the silicon mass increases. The actual energy of the phonon mode is given by the separation between this peak and the ZPL, and therefore the phonon energy decreases for ^{29}Si and ^{30}Si. The calculated phonon energies for this feature are 63.76 ± 0.06 meV for ^{28}Si, 62.74 ± 0.06 meV for ^{29}Si, and 61.55 ± 0.06 meV for ^{30}Si. The intensities of the ZPL and the sideband spectra cannot be compared since the acquisition was done with different gratings. (c) The 128 meV peak does not shift systematically with isotope, and in particular it does not match the expected position for a second harmonic of the local mode (dashed line).

silicon isotope present in a given SiV$^-$ centre. This is the first observation of SiV$^-$ isotopic shift at the single-site level, and indicates that the silicon isotope present in an individual SiV$^-$ site can be unambiguously identified. The 'digital shift' between distinct SiV$^-$ sites is an elegant confirmation of the isotopic explanation presented for the 12-line structure seen in ensembles [25].

The average ZPL spectrum for each silicon isotope is shown in figure 3(a). The fine structure splittings are identical for each isotope, but the ^{29}Si and ^{30}Si ZPLs are shifted to longer wavelengths by 0.16 nm (87 GHz, 0.35 meV) and 0.30 nm (166 GHz, 0.66 meV) respectively. These isotopic shifts of the ZPL for ^{29}Si and ^{30}Si are in close correspondence with the values previously observed in ensemble measurements [25].

It is also of interest to examine the phonon sideband for isotopic shift. Since the sideband features are much broader than the ZPL, small shifts are impossible to resolve in ensemble measurements which simultaneously record all isotopes. Any isotopic shift would therefore appear as imperceptible broadening in ensemble spectra. With the ability to identify the silicon isotope present in individual SiV$^-$ centres we are able for the first time to examine the phonon sideband for isotopic variation. The only other feature in the PL spectrum that exhibited measurable isotopic shift was the 64 meV phonon peak, shown in figure 3(b). This feature moves to shorter wavelength meaning that the phonon energy, which is determined by the separation from the ZPL, is decreasing with heavier isotopes.

4. Identification and discussion of a local vibrational mode

It is possible to calculate the precise energy of this phonon peak for each of the silicon isotopes by determining its distance from the corresponding ZPL. From the spectra shown in figure 3(b) the phonon energies were found to be $E_{28} = 63.76 \pm 0.06$ meV, $E_{29} = 62.74 \pm 0.06$ meV, and $E_{30} = 61.55 \pm 0.06$ meV for ^{28}Si, ^{29}Si, and ^{30}Si respectively. These give the ratios

$$\frac{E_{28}}{E_{29}} = 1.0163 \pm 0.0014 \quad \approx \quad 1.0177 = \sqrt{\frac{m_{29}}{m_{28}}} \tag{1}$$

and

$$\frac{E_{28}}{E_{30}} = 1.0359 \pm 0.0011 \quad \approx \quad 1.0357 = \sqrt{\frac{m_{30}}{m_{28}}}. \tag{2}$$

As indicated in the right hand column, the measured ratios are in close agreement with a simple harmonic oscillator model where the phonon frequency ω is given by

$$\omega = \sqrt{\frac{k}{m}} \tag{3}$$

for spring constant k and an oscillating mass m corresponding to the silicon atom. The validity of this simple model indicates that the 64 meV spectral feature arises from an oscillation of the silicon atom without much participation of the carbon nuclei forming the diamond lattice. Therefore, it must be a local vibrational mode of the SiV^- centre.

This conclusion informs an ongoing discussion about this feature in the SiV^- sideband, and resolves some contention. Early in the analysis of the SiV^- sideband it was suggested that the peak at 42 meV is due to a local vibrational mode, and that the other features arise from the lattice [26]. In contrast, Gorokhovsky *et al* [27] showed that 64 meV was close to a phonon energy in silicon and concluded that this SiV^- feature was a local mode. They also suggested the feature at 128 meV could be a second harmonic of this vibration. More recently it has been proposed that either the 42 meV or the 64 meV features could arise from a local mode, depending on the symmetry of the defect [28]. We have shown conclusively that the 64 meV sideband feature is due to a local vibrational mode. Our spectral measurements did not show any isotopic variation in the 42 meV feature, although it is significantly broader and so small shifts in position would be difficult to detect. Additionally, broad peaks do not generally arise from local modes, and therefore we conclude the 42 meV feature to be non-localized.

If the 128 meV feature was a second harmonic of the 64 meV local mode then it would be expected to exhibit twice the isotopic shift of the 64 meV peak. This expected shift is illustrated by the dashed line in figure 3(c), and it is clear that the measured peak at 128 meV does not follow this behaviour. Therefore we conclude that this peak is not due to a harmonic of the local mode at 64 meV and is not a local mode itself.

Numerous extra electronic transitions have been proposed to account for the photon autocorrelation statistics of SiV^-, which exhibit bunching shoulders typical of storage in metastable states [29]. An additional electronic transition has been reported at 822.7 nm [30], although this spectral feature was not observed in our measurements here. Since we have shown that the 64 meV feature is due to a local vibrational mode, it cannot be due to an electronic transition associated with metastable states. We conclude that the 64 meV sideband peak does not give insight into the storage mechanism.

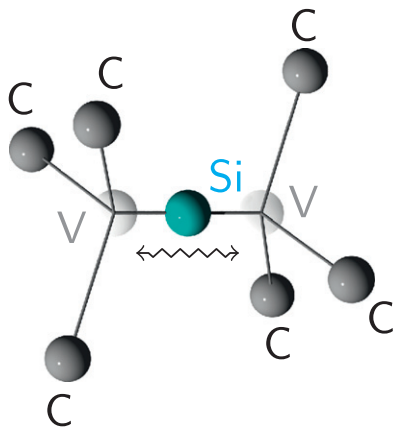

Figure 4. The D_{3d} symmetry of SiV^- with the oscillating silicon atom. Carbon (C) atoms are marked in grey, while silicon (Si) is symbolized in cyan. For clarity the vacant lattice positions are marked by transparent spheres and the label 'V', even though the conventional description of this defect is as a substitutional silicon and a single vacancy that then relaxes into this split-vacancy configuration. This symmetry supports a localized oscillation of the silicon atom along the ⟨111⟩ axis of the diamond host lattice.

It is widely accepted that SiV^- has D_{3d} symmetry [22–24], which consists of the silicon atom in the middle of a split vacancy as shown in figure 4. The neutrally charged SiV^0 centre was established to have D_{3d} symmetry by magnetic resonance measurements. Although magnetic resonance has not been observed for the negative charge state, this structure was proposed for SiV^- from *ab initio* calculations [24]. It is worthwhile considering the implications of a local silicon vibration within this geometry. The 64 meV peak is polarized similarly to the ZPL and has most of its strength coming from the axial dipole moment [23]. This suggests that the silicon atom oscillates along the ⟨111⟩ symmetry axis. Since the silicon atom lies between two vacant lattice sites, its position on this axis is weakly confined. Such a geometry is likely to support an oscillation of the silicon atom that does not involve motion of the carbon nuclei.

5. Discussion of mechanism for ZPL isotopic shift

Although the isotopic shift of the SiV^- ZPL has been known since the early ensemble measurements of Clark *et al* [25], a mechanism for this shift has never been proposed. Our observation of a local vibrational mode provides a plausible explanation, following the direction of Iakoubovskii and Davies [31] for the 1.4 eV optical centre and Lawson *et al* [32] for the H2 centre. The key idea is to consider that the ZPL includes transitions between phonon states as long as they involve the same phonon occupation in the ground and excited states. In such a case there is no loss or gain of phonons and so the transition contributes to the ZPL. If the curvature of the vibrational potential differs between the ground and excited states, then levels of matching phonon occupation will not be at the same energy and this energy difference will contribute to the energy of the observed ZPL transition.

We have observed a local mode for SiV^- which could interact with the ZPL in this manner to explain the isotopic shift of the ZPL. The ZPL energy $h\nu$ in this model can be expressed in the form

$$h\nu = h\nu_{\mathrm{el}} + \sum_{i}^{N}\left(n_i + \frac{1}{2}\right)\hbar\left(\omega_i' - \omega_i\right) \tag{4}$$

following Lawson *et al* [32]. Here $h\nu_{\mathrm{el}}$ is the purely electronic transition energy. The term in the sum is the energy difference between the excited (ω') and ground (ω) states of the ith phonon mode (which could be a local vibration) at the same occupation level n_i. Transitions of this kind between levels of matching phonon occupation contribute to the ZPL since phonons are not involved [31]. This energy is summed over all N phonon modes that couple to electronic states. At zero temperature only the $n_i = 0$ levels will be occupied, while at higher temperatures energy levels with increasing n_i occur providing a broadening of the ZPL [31].

We do not know which global modes are involved in the sum, but do know that one of the vibrational modes is entirely local. Because this vibration behaves exactly as a harmonic oscillator, and therefore does not involve the carbon atoms of the diamond lattice, it is possible to separate local modes out from the sum. The sum over all phonons can hence be separated into independent sums over the local vibrational modes of the silicon atom and over the phonons which involve the carbon lattice. So equation (4) becomes

$$h\nu = h\nu_{\mathrm{el}} + \sum_{i}^{M}{}_{\mathrm{Si}}\left(n_i + \frac{1}{2}\right)\hbar\left(\omega_i' - \omega_i\right) + \sum_{i}^{N-M}{}_{\mathrm{C}}\left(n_i + \frac{1}{2}\right)\hbar\left(\omega_i' - \omega_i\right). \tag{5}$$

The Si subscripted sum covers the M local silicon modes, while the subscript C sums over the $N - M$ carbon phonons. To see if this model is valid to explain the shift of the ZPL, the energy ratios between the isotopes are now compared.

As we have established in the previous section, changing the silicon mass only affects the energy of the local phonons which change as $\omega \propto 1/\sqrt{m}$. Therefore the only changing term is the sum over the local silicon phonons, and so this term gives the differences $\Delta E_{28,29}$ and $\Delta E_{28,30}$. The frequencies (ω_i and ω_i') of the ^{29}Si and ^{30}Si can be expressed in relation to ^{28}Si by the fraction of the square roots of the masses. This allows the energy difference to be expressed as:

$$\Delta E_{28,29} = \hbar\left(1 - \sqrt{m_{28}/m_{29}}\right)\cdot\left(\sum_{i}^{M}{}_{^{28}\mathrm{Si}}\left(n_i + \frac{1}{2}\right)\hbar\left(\omega_i' - \omega_i\right)\right) \tag{6}$$

and similarly for $\Delta E_{28,30}$. The ratio between these energy differences is then

$$\frac{\Delta E_{28,29}}{\Delta E_{28,30}} = \frac{1 - \sqrt{m_{28}/m_{29}}}{1 - \sqrt{m_{28}/m_{30}}} \approx 0.51. \tag{7}$$

Since we have measured the ZPL energy shift for all three silicon isotopes this model can be compared to our experiments presented in figure 3. The theoretical ratio is in close agreement with the empirically determined value of 0.52 ± 0.07.

The correspondence between theory and experiment suggests there is validity to this model and that the shift of the ZPL with different isotopes arises from the presence of local modes. Without knowing the difference in curvature of the harmonic potentials between the ground and excited states, the model is unable to predict the direction of the ZPL shift. We have experimentally found that the ZPL moves to lower energy as the silicon mass increases, and this observation may assist theoretical efforts to describe the phonon harmonic potentials.

6. Conclusion

We have demonstrated the ability to unambiguously identify the silicon isotope contained in a single SiV^- centre from the PL spectra. This ability is of interest because it allows easy identification of centres containing ^{29}Si. Only these centres provide the possibility of accessing silicon nuclear spin, which is a feature of interest for quantum information applications. Nuclear spins in diamond are weakly coupled to their environment and generally have long coherence times which are necessary for quantum information storage.

We identify the 64 meV phonon sideband feature to be a local vibrational mode of the silicon atom. This resolves contention about local modes in the literature [26–28] and gives insight into the vibrational properties of SiV^-. The presence of a local mode suggests a plausible explanation for the ZPL isotopic shift. Although the D_{3d} symmetry of SiV^- is widely accepted, it has not been directly observed. The local vibrational mode we have described here is entirely consistent with D_{3d} symmetry and this result provides further indirect evidence supporting this split-vacancy defect geometry.

Acknowledgments

The authors acknowledge funding from EU (DIAMANT, SIQS, DIADEMS, EQUAMS), ERC, German Science Foundation—DFG (SFB TR21, FOR1482, FOR1493), JST, JSPS KAKENHI (No. 26246001), DARPA, Sino-German Center, VW Stiftung and ARC (EQUS). We thank Marcus Doherty for helpful discussions.

References

[1] Gruber A, Dräbenstedt A, Tietz C, Fleury L, Wrachtrup J and von Borczyskowski C 1997 Scanning confocal optical microscopy and magnetic resonance on single defect centers *Science* **276** 2012–4

[2] Wang C, Kurtsiefer C, Weinfurter H and Burchard B 2006 Single photon emission from SiV centres in diamond produced by ion implantation *J. Phys. B: At. Mol. Opt. Phys.* **39** 37

[3] Kurtsiefer C, Mayer S, Zarda P and Weinfurter H 2000 Stable solid-state source of single photons *Phys. Rev. Lett.* **85** 290–3

[4] Rogers L J *et al* 2014 Multiple intrinsically identical single-photon emitters in the solid state *Nat. Commun.* **5** 4739

[5] Knill E, Laflamme R and Milburn G J 2001 A scheme for efficient quantum computation with linear optics *Nature* **409** 46–52

[6] Wrachtrup J and Jelezko F 2006 Processing quantum information in diamond *J. Phys.: Condens. Matter* **18** 807–24

[7] Childress L, Taylor J M, Sørensen A S and Lukin M D 2006 Fault-tolerant quantum communication based on solid-state photon emitters *Phys. Rev. Lett.* **96** 070504

[8] Maletinsky P, Hong S, Grinolds M S, Hausmann B, Lukin M D, Walsworth R L, Loncar M and Yacoby A 2012 A robust scanning diamond sensor for nanoscale imaging with single nitrogen-vacancy centres *Nat. Nanotechnol.* **7** 320–4

[9] Ermakova A *et al* 2013 Detection of a few metallo-protein molecules using color centers in nanodiamonds *Nano Lett.* **13** 3305–9

[10] Fu C-C *et al* 2007 Characterization and application of single fluorescent nanodiamonds as cellular biomarkers *Proc. Natl Acad. Sci.* **104** 727–32

[11] Vlasov I I *et al* 2013 Molecular-sized fluorescent nanodiamonds *Nat. Nanotechnology* **9** 54–58

[12] Vlasov I I, Barnard A S, Ralchenko V G, Lebedev O I, Kanzyuba M V, Saveliev A V, Konov V I and Goovaerts E 2009 Nanodiamond photoemitters based on strong narrow-band luminescence from silicon-vacancy defects *Adv. Mater.* **21** 808–12
[13] Neu E, Steinmetz D, Riedrich-Möller J, Gsell S, Fischer M, Schreck M and Becher C 2011 Single photon emission from silicon-vacancy colour centres in chemical vapour deposition nano-diamonds on iridium *New J. Phys.* **13** 025012
[14] Sipahigil A, Jahnke K D, Rogers L J, Teraji T, Isoya J, Zibrov A S, Jelezko F and Lukin M D 2014 Indistinguishable photons from separated silicon-vacancy centers in diamond *Phys. Rev. Lett.* **113** 113602
[15] Müller T, Hepp C, Pingault B, Neu E, Gsell S, Schreck M, Sternschulte H, Steinmüller-Nethl D, Becher C and Atatüre M 2014 Optical signatures of silicon-vacancy spins in diamond *Nat. Commun.* **5** 3328
[16] Rogers L J *et al* 2014 All-optical initialization, readout, and coherent preparation of single silicon-vacancy spins in diamond arXiv:1410.1355
[17] Childress L, Gurudev Dutt M V, Taylor J M, Zibrov A S, Jelezko F, Wrachtrup J, Hemmer P R and Lukin M D 2006 Coherent dynamics of coupled electron and nuclear spin qubits in diamond *Science* **314** 281–5
[18] Jacques V, Neumann P, Beck J, Markham M, Twitchen D, Meijer J, Kaiser F, Balasubramanian G, Jelezko F and Wrachtrup J 2009 Dynamic polarization of single nuclear spins by optical pumping of nitrogen-vacancy color centers in diamond at room temperature *Phys. Rev. Lett.* **102** 057403
[19] Dutt M V G, Childress L, Jiang L, Togan E, Maze J, Jelezko F, Zibrov A S, Hemmer P R and Lukin M D 2007 Quantum register based on individual electronic and nuclear spin qubits in diamond *Science* **316** 1312–6
[20] Gali A and Maze J R 2013 An *ab initio* study on split silicon-vacancy defect in diamond: electronic structure and related properties *Phys. Rev.* B **88** 235205
[21] Neu E, Hepp C, Hauschild M, Gsell S, Fischer M, Sternschulte H, Steinmüller-Nethl D, Schreck M and Becher C 2013 Low-temperature investigations of single silicon vacancy colour centres in diamond *New J. Phys.* **15** 043005
[22] Hepp C *et al* 2014 Electronic structure of the silicon vacancy color center in diamond *Phys. Rev. Lett.* **112** 036405
[23] Rogers L J *et al* 2014 Electronic structure of the negatively charged silicon-vacancy center in diamond *Phys. Rev.* B **89** 235101
[24] Goss J P, Jones R, Breuer S J, Briddon P R and Öberg S 1996 The twelve-line 1.682 eV luminescence center in diamond and the vacancy-silicon complex *Phys. Rev. Lett.* **77** 3041–4
[25] Clark C D, Kanda H, Kiflawi I and Sittas G 1995 Silicon defects in diamond *Phys. Rev.* B **51** 16681–8
[26] Feng T and Schwartz B D 1993 Characteristics and origin of the 1.681 eV luminescence center in chemical-vapor-deposited diamond films *J. Appl. Phys.* **73** 1415–25
[27] Gorokhovsky A A, Turukhin A V, Alfano R R and Phillips W 1995 Photoluminescence vibrational structure of si center in chemical vapor deposited diamond *Appl. Phys. Lett.* **66** 43–45
[28] Zaitsev A M 2000 Vibronic spectra of impurity-related optical centers in diamond *Phys. Rev.* B **61** 12909–22
[29] Neu E, Agio M and Becher C 2012 Photophysics of single silicon vacancy centers in diamond: implications for single photon emission *Opt. Express* **20** 19956–71
[30] Neu E, Albrecht R, Fischer M, Gsell S, Schreck M and Becher C 2012 Electronic transitions of single silicon vacancy centers in the near-infrared spectral region *Phys. Rev.* B **85** 245207
[31] Iakoubovskii K and Davies G 2004 Vibronic effects in the 1.4-eV optical center in diamond *Phys. Rev.* B **70** 245206
[32] Lawson S C, Davies G, Collins A T and Mainwood A 1992 The 'H2' optical transition in diamond: the effects of uniaxial stress perturbations, temperature and isotopic substitution *J. Phys.: Condens. Matter* **4** 3439–52
[33] Alkauskas A, Buckley B B, Awschalom D D and Van de Walle C G 2014 First-principles theory of the luminescence lineshape for the triplet transition in diamond NV centre *New J. Phys.* **16** 073026
[34] Edmonds A, Newton M, Martineau P, Twitchen D and Williams S 2008 Electron paramagnetic resonance studies of silicon-related defects in diamond *Phys. Rev.* B **77** 081201